



# Lateralizing the affected side of hippocampal sclerosis with quantitative high angular resolution diffusion scalars: a preliminary approach validated by diffusion spectrum imaging

Yi-He Wang<sup>1#</sup>, Zhen-Ming Wang<sup>2#</sup>, Peng-Hu Wei<sup>1</sup>, Chao Lu<sup>1</sup>, Xiao-Tong Fan<sup>1</sup>, Lian-Kun Ren<sup>3</sup>, Yong-Zhi Shan<sup>1</sup>, Jie Lu<sup>2,4</sup>, Guo-Guang Zhao<sup>1,5^</sup>

<sup>1</sup>Department of Neurosurgery, Xuanwu Hospital, Capital Medical University, Beijing, China; <sup>2</sup>Department of Radiology, Xuanwu Hospital, Capital Medical University, Beijing, China; <sup>3</sup>Department of Neurology, Xuanwu Hospital, Capital Medical University, Beijing, China; <sup>4</sup>Department of Nuclear Medicine, Xuanwu Hospital, Capital Medical University, Beijing, China; <sup>5</sup>Center of Epilepsy, Beijing Institute for Brain Disorder, Beijing, China

**Contributions:** (I) Conception and design: J Lu, GG Zhao; (II) Administrative support: GG Zhao, LK Ren, YZ Shan; (III) Provision of study materials or patients: YH Wang, ZM Wang; (IV) Collection and assembly of data: YH Wang, PH Wei, C Lu, XT Fan; (V) Data analysis and interpretation: YH Wang, ZM Wang, PH Wei; (VI) Manuscript writing: All authors; (VII) Final approval of manuscript: All authors.

<sup>#</sup>These authors contributed equally to this work.

**Correspondence to:** Jie Lu; Guo-Guang Zhao. Department of Neurosurgery, Xuan Wu Hospital, Capital Medical University, No. 45, Changchun Street, Xuanwu District, Beijing 100053, China. Email: [imaginglu@hotmail.com](mailto:imaginglu@hotmail.com); [ggzhao@vip.sina.com](mailto:ggzhao@vip.sina.com).

**Background:** Conflicts in regarding the lateralization of the seizure onset for mesial temporal lobe epilepsy (MTLE) are frequently encountered during presurgical evaluation. As a more elaborate, quantified protocol, indices of diffusion spectrum imaging (DSI) might be sensitive to evaluate the seizure involvement. However, the accuracy was less revealed. Herein, we determined the lateralizing value of the DSI indices among MTLE patients.

**Methods:** Eleven MTLE patients were enrolled together with 11 matched health contrasts. All the participants underwent a DSI scan and with reconstruction of the diffusion scalar, including quantitative anisotropy (QA), isotropic (ISO), and track density imaging (TDI) values. Statistics of these indices were applied to identify the differences between the healthy and ipsilateral sides, and those between the patients and the controls, with special attention to areas of the crura of fornix (FORX), the parahippocampal radiation of the cingulum (PHCR), the hippocampus (HP), parahippocampus (PHC), amygdala (AM) and entorhinal cortex (EC).

**Results:** Regarding lateralization, TDI of the FORX and the PHCR reached an AUC value of 0.95 and 0.93, respectively ( $P < 0.05$ ), and QA, ISO, TDI of the PHCR, as well as TDI of the FORX were statistically significant amongst the laterals of the patients ( $P < 0.05$ ). Also, the QA of the PHCR were statistically different in the patients' ipsilateral side relative to the contrasts ( $P < 0.017$ ). The diffusion level on different grey matter structures were significantly decreased including HP, AM and EC in GQI space ( $P < 0.017$ ).

**Conclusions:** The quantitative diffusion scalars of the DSI, especially TDI of the FORX and the PHCR, are sensitive indices to define the ipsilateral side for MTLE patients. For preliminary exploration, the use of quantitative DSI scalars may help to improve the seizure outcome by increasing the accuracy of localization and lateralization for MTLE.

**Keywords:** Diffusion spectrum imaging (DSI); mesial temporal lobe epilepsy (MTLE); high angular quantitative analysis

Submitted Aug 06, 2020. Accepted for publication Nov 30, 2020.

doi: [10.21037/atm-20-5719](https://doi.org/10.21037/atm-20-5719)

**View this article at:** <http://dx.doi.org/10.21037/atm-20-5719>

<sup>^</sup> ORCID: [0000-0002-7569-5252](https://orcid.org/0000-0002-7569-5252).

## Introduction

Mesial temporal lobe epilepsy (MTLE) is one of the most common types of human epilepsy. Presurgical evaluation is of immense importance in patients with MTLE because surgical treatment can provide seizure relief in 60–80% of the patients. However, 30–40% of patients with MTLE show negative magnetic resonance imaging (MRI) results, and the lateralization of the seizure in 1–15% cannot be determined only with scalp electroencephalogram (EEG) and MRI. It is necessary to optimize the noninvasive presurgical evaluation workflow for MTLE patients to provide less invasive surgery and better seizure outcome.

Comprehensive imaging modalities including functional imaging and structural imaging can provide lateralization or localization information for MTLE. Among them, diffusion MRI (dMRI) has played an important role in the presurgical evaluation of MTLE; it helps to determine the microstructural damage caused by neuronal loss at the seizure onset zone and allows the identification of the extra-focal regions connected to the seizure focus to be determined (1). Diffusion tensor imaging (DTI) has been widely used in the presurgical evaluation of patients with unilateral MTLE to assess the diffusion asymmetry between the two hemispheres (1–6). Nazem-Zadeh *et al.* have developed an important DTI-based response-driven lateralization model for MTLE, which helps to reduce diagnostic errors when determining laterality (7). However, DTI as one of the model-based methods cannot help determine the crossing and termination of fibers, and also generates multiple artifacts and false tracts, which may decrease its accuracy in the clinical settings (8).

Diffusion spectrum imaging (DSI) has been developed as a new, model-free method based on high angular resolution imaging, which can overcome the limitations of DTI (9,10). Preliminary experiments with this procedure have showed the similarity of neuroanatomical features between primates and human (10,11). Compared with DTI, DSI improves quantitative resolution with intra-voxel diffusion heterogeneity and does not resolve the average direction difference; moreover, to some extent, DSI quantifies the diffusion level more precisely than other methods. There are limited studies using DSI in the presurgical evaluation of the patients with MTLE. To the best of our knowledge, there were no reports using this high-resolution technique to investigate the heterogeneity of gray and white matter between the two sides of unilateral MTLE. In this study, we intend to (I) use DSI to quantitatively compare the

microstructural differences of gray and white matter of the two sides in MTLE and (II) assess the reliability and effectiveness of DSI in lateralizing MTLE during presurgical evaluation. We present the following article in accordance with the STROBE reporting checklist (available at <http://dx.doi.org/10.21037/atm-20-5719>).

## Methods

### *Patients and controls*

A series of MTLE patients were recruited following the specific inclusion and exclusion criteria. The inclusion criteria were as follows: (I) unilateral MTLE, (II) DSI acquired with the same protocol, (III) diagnosis of MTLE by a multidisciplinary team (MDT) or postoperative pathology. The exclusion criteria were bilateral MTLE or other types of temporal lobe epilepsy and lack of DSI acquisition.

All the included patients have received the same presurgical evaluation. First, DSI and three-dimensional (3D) MRI imaging were performed after long-term video scalp EEG examination and detailed semiology investigation. Then, unilateral MTLE was defined by an MDT for both lateralization and localization. Finally, anterior temporal lobectomy (ATL) or stereoelectroencephalography (SEEG)-guided radiofrequency thermocoagulation performed in these patients with unilateral MTLE. The final diagnosis was determined by MDT discussion or by SEEG results or pathological results.

For the control group, the inclusion criteria were as follows: (I) none of the controls had neurological or psychotropic disorders, (II) all the controls underwent the DSI scan following the same protocol, (III) age and sex be matched with the patient group. The exclusion criteria were healthy controls who did not agree to recruit or those with neurological or psychotropic disorders. A brief description of the characteristics of both patients and controls is presented in *Table 1*.

The study was conducted in accordance with the Declaration of Helsinki (as revised in 2013). The study was approved by the ethics committee at Xuanwu Hospital (NO. LYS [2019] 097) and informed consent was taken from all the patients.

### *MRI and DSI acquisition*

All the raw data related to this study were acquired

**Table 1** Clinical data of the patients and controls

Pt.	Sex	Age (y)	Handedness	Age at first seizure	History	Types	Frequency	PET Re-sults	No. of AEDs	EEG (side/region)	SEEG	MDT	Pathology
MTLE patients													
1	F	38	L	15	-	FBTCS/FIAS	1-2/W	L/T	2	L/T	L	LHS	/
2	F	22	L	13	-	FBTCS	1-2/M	L/T, P	3	L/T, F	-	LHS	HS
3	F	18	L	4	-	FBTCS/FIAS	2-3/D	R/T, F, P	4	B/T	-	RHS	HS
4	M	14	L	2	-	FBTCS/FIAS	2-3/W	L/T, F	3	L/T	-	LHS	HS
5	M	33	L	13	-	FBTCS/FIAS	3-5/D	R/T	3	R/T, F	-	RHS	HS
6	M	48	L	18	-	FIAS	2-3/D	R/T, F	3	R/T	-	RHS	/
7	F	15	L	4	-	FIAS	2-4/D	L/T, P, O	3	L/T, F	-	LHS	HS
8	M	33	L	13	-	FBTCS	1-2/M	R/T, P	3	R/T, F	-	RHS	HS
9	F	36	L	26	-	FIAS	3-4/M	L/T, F, P	4	L/T	-	LHS	HS
10	M	22	L	10	-	FBTCS/FIAS	1-2/M	L/T	3	B/T, F	-	LHS	HS
11	M	32	L	9	-	FIAS	2-3/W	L/T	4	L/T	-	LHS	HS
Normal controls													
1	M	25	L	-	None	-	-	-	-	-	-	-	-
2	M	30	L	-	None	-	-	-	-	-	-	-	-
3	M	21	L	-	None	-	-	-	-	-	-	-	-
4	F	21	L	-	None	-	-	-	-	-	-	-	-
5	F	24	L	-	None	-	-	-	-	-	-	-	-
6	F	30	L	-	None	-	-	-	-	-	-	-	-
7	M	29	L	-	None	-	-	-	-	-	-	-	-
8	M	24	L	-	None	-	-	-	-	-	-	-	-
9	F	27	L	-	None	-	-	-	-	-	-	-	-
10	F	24	L	-	None	-	-	-	-	-	-	-	-
11	M	21	L	-	None	-	-	-	-	-	-	-	-

MTLE, mesial temporal lobe epilepsy; M, male; F, female; L, left; R, right; FBTCS, focal to bilateral tonic-clonic seizure; FIAS, focal impaired awareness seizure; B, bilateral; T, temporal area; F, frontal area; P, parietal area; O, occipital area; W, week; M, month; D, day; HS, hippocampal sclerosis. The side and the area of the EEG region were determined by the interictal scalp EEG.

using the same scanner (GE SIGNA Premier, General Electric Healthcare, Waukesha, WI, USA) at Xuanwu Hospital.

The 3D MRI (T1-Weighted 3D magnetization prepared rapid acquisition gradient echo sequence, T1W1-3D-MPRAGE) scanning parameters and conditions were as follows: slice thickness = 1 mm; repetition time (TR) = 2,420 ms; echo time (TE) = 2.376 ms; inversion time = 900 ms; field of view = 512 mm × 512 mm; number of excitations = 1, and acquisition time = 6 min.

The DSI scanning (half-q-space DSI with 256 directions) parameters and conditions were as follows: 64 channel head coils, b values range from 0 to 7,000 s/mm<sup>2</sup>; TR = 5,548 ms; TE = 84.1 ms; voxel size = 2 mm × 2 mm × 2 mm; layer thickness = 2 mm; imaging field = 112 mm × 112 mm, flip angle = 90°; parallel acquisition acceleration value = 2; phase coding acceleration value = 3; and acquisition time = 26 min. The data processing and quality control were assessed by two experienced radiologists, while ensuring no head motion or other processing errors.

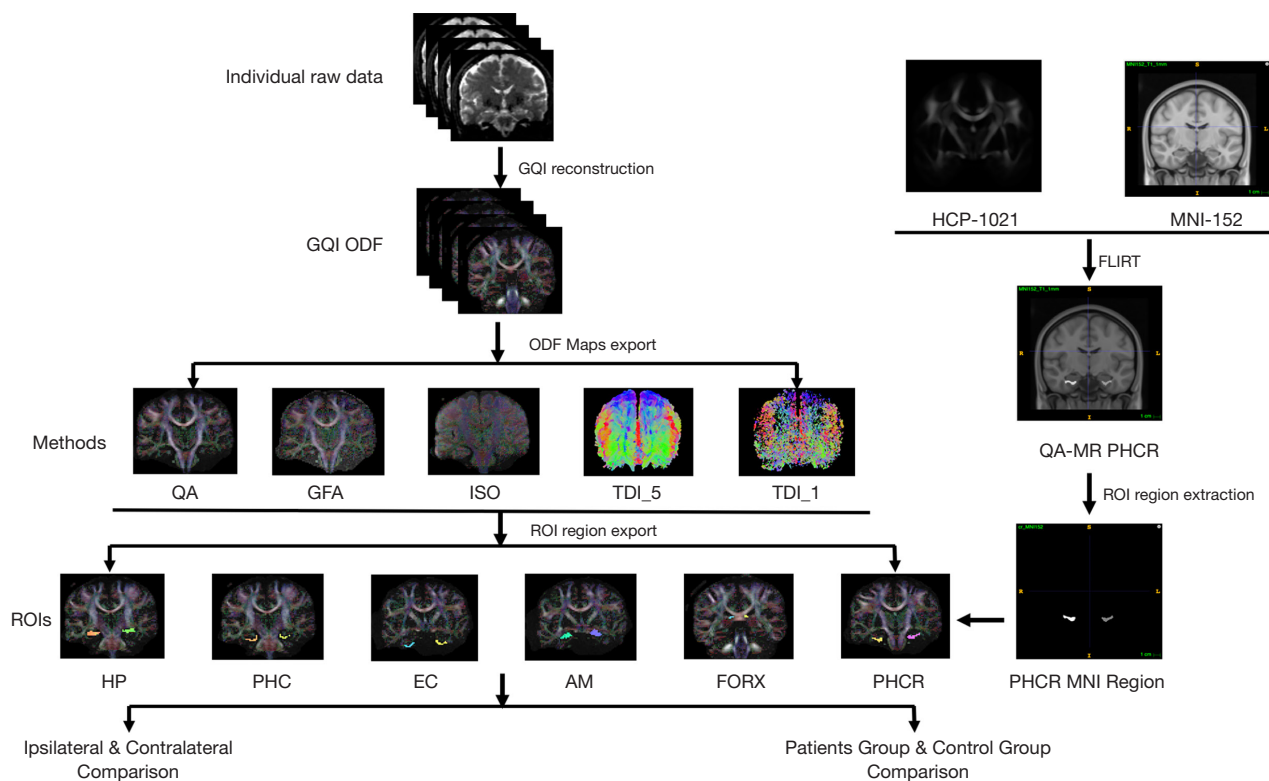


**Figure 1** Raw data pre-processing flow chart. All raw data collections followed the same workflow. This chart demonstrates the process of diffusion scalar derivation, region of interest (ROI) exportation and quantitative analysis. Orientation distribution functions (ODF) maps for the 22 individuals were first reconstructed following the generalized q-sampling imaging (GQI) algorithm. ROIs were exported from DSI-studio followed by the quantitative comparison.

### Raw data pre-processing

All data reconstruction was performed with DSI-Studio software (<http://dsi-studio.labsolver.org>). Post-reconstruction quality check was performed using the DSI-Studio software to confirm the absence of registration error ( $R > 0.6$ ). Each voxel and the orientation distribution functions (ODF) were extracted with the generalized q-sampling imaging (GQI) algorithm for individual comparison (12). The reconstruction parameters for reconstruction were as follows: CSF calibration selected, diffusion sampling length ratio: 1.10; ODF tessellation: 20 folds; and number of fibers resolved: 10. A total of 22 individual representations of the ODF map in GQI space were created using the quantitative anisotropy (QA) and isotropic (ISO) values of each individual DSI data (Figure 1).

Track density imaging (TDI) value was another scalar in this study. It provides a relatively novel and quantitative method to produce high-quality white matter images

with high spatial resolution (13-15). For each TDI reconstruction, the individual tracking threshold was set at 60% of the maximum value with MATLAB R2018a (Mathworks, Natick, Mass, USA). Whole brain seeding was processed with an angular threshold of  $90^\circ$ . For gray matter, the step size was 0.1, minimum (Min) length = 0 mm, and maximum (Max) length = 5 mm. For white matter fiber bundles, the step size was 0.5, Min length = 5 mm, Max length = 300 mm, the fiber tracking stopped when the maximum number of seeds was 2,000,000 (Figure 1).

### Region of interest (ROI) selection and extraction

In this study, the bilateral hippocampus (HP), parahippocampus (PHC), amygdala (AM), and entorhinal cortex (EC) were the main gray matter structures examined, and for white matter, the crus of fornix (FORX) and the parahippocampal radiation of the cingulum (PHCR) were selected to compare the heterogeneity of the examined

scalars between the two sides of MTLE patients and controls.

For HP, PHC, AM, and EC, the ROI in GQI space can be exported and saved from the embedded template in DSI studio software. As for bilateral FORX, fiber tracking and reconstruction methods were used, and calculated region was restricted only to the crus of the bilateral fornix. The tracking parameters were as follows: step size =0.1, angular threshold =90°, Min length =5 mm, and Max length =300 mm. The fiber tracking stopped when the maximum number of seeds was 50,000. The FORX in GQI space were then exported (*Figure 1*).

For PHCR, the module of segmentation editor used was 3D Slicer software (<https://www.slicer.org>). The QA map in the Montreal Neurological Institute (MNI) region was first created using Functional Magnetic Resonance Imaging of the Brain (FMRIB) Linear Image Registration Tool (FLIRT) in FSL (FMRIB Software Library) combining the MNI152 ([http://nist.mni.mcgill.ca/?page\\_id=714](http://nist.mni.mcgill.ca/?page_id=714)) template and the HCP1201 (<http://brain.labsolver.org/diffusion-mri-templates/hcp-842-hcp-1021>) template. The diffusion MR map in MNI space was then used in 3D Slicer to restrict the threshold with only the white matter visible (no gray matter). The visualized white matter regions adjacent to the PHC were extracted as PHCR with a comparable length to the PHC. Finally, the bilateral PHCR in the MNI space was imported to DSI-Studio software and exported as ROIs in GQI space (*Figure 1*).

### Quantitative analysis of ROIs

As the patients included herein had a definitive diagnosis of MTLE, the capability of FORX and PHCR to determine lateralization was assessed in our study. The bilateral QA, ISO and TDI values of the FORX and PHCR were compared between the ipsilateral side (the side with MTLE) and the contralateral side using Paired *t*-test or the Wilcoxon test if the data set did not fit the normal distribution. The comparison between the two ROIs were further investigated among the ipsilateral side, contralateral side, and the controls separately. Finally, in order to observe whether FORX\_TDI and PHCR\_TDI can be lateralized for MTLE, a descriptive analysis of the sensitivity and specificity between the two structures were compared in lateralization of MTLE using receiver operating characteristic (ROC) curve.

The quantitative analysis for gray matter structures was conducted between the HP, PHC, AM and EC. The

heterogeneity between the bilateral mesial temporal areas in patients with MTLE were first processed. The four ipsilateral ROIs were compared to each other and  $P < 0.05$  was considered statistically significant. The bilateral side of the four ROIs were compared separately with the control data collected from the volunteers. Specificity was calculated between them with the Independent-samples *t*-test or the Mann-Whitney U test. Significant level  $\alpha$  ( $\alpha = 0.05$ ) was adjusted as 0.017 using Bonferroni method in order to avoid Type I error when performed multiple comparisons of QA and ISO among ipsilateral and contralateral values, and controls. TDI values were only compared between ipsilateral and contralateral regions, thus the level  $\alpha$  was determined as 0.05.

### Statistical analysis

All statistical analyses were performed with the Solutions Statistical Package for the Social Sciences (SPSS, Version 22; IBM, Armonk, New York, USA). The figures in our study were editing and drawing using Photoshop (Version CC 2019 for Mac, Adobe Systems Incorporated, San Jose, USA) and GraphPad Prism (Version 8.0 for Mac, GraphPad Software, San Diego, USA).

## Results

### General information

In this study, we recruited 11 patients (6 men and 5 women, age:  $28.3 \pm 10.8$  years) with unilateral medial temporal lobe epilepsy (7 left and 4 right) from the Department of Neurosurgery in Xuanwu Hospital between May 2019 and January 2020. In these 11 patients, we observed a series of abnormal discharges during the interictal phase. Most of the patients have a lateralization on the scalp-EEG results with some of the patients showing bilateral asynchronous discharges during the ictal and interictal period (*Table 1* and *Figure 2*). All the patients had a definite diagnosis of MTLE after intensive discussion by the MDT consisting of a neurosurgeon, a neurologist, and a radiologist. The seizure type of the 11 patients were listed according to the 2017 ILAE classification, all the patients suffered from the focal onset with FBTCS (focal to bilateral tonic-clonic seizure) and/or FIAS (focal impaired awareness seizure) (16).

Among the 11 patients included, nine underwent a standard ATL with a clear pathology diagnosis of HP sclerosis (*Table 1*). One patient underwent the implantation

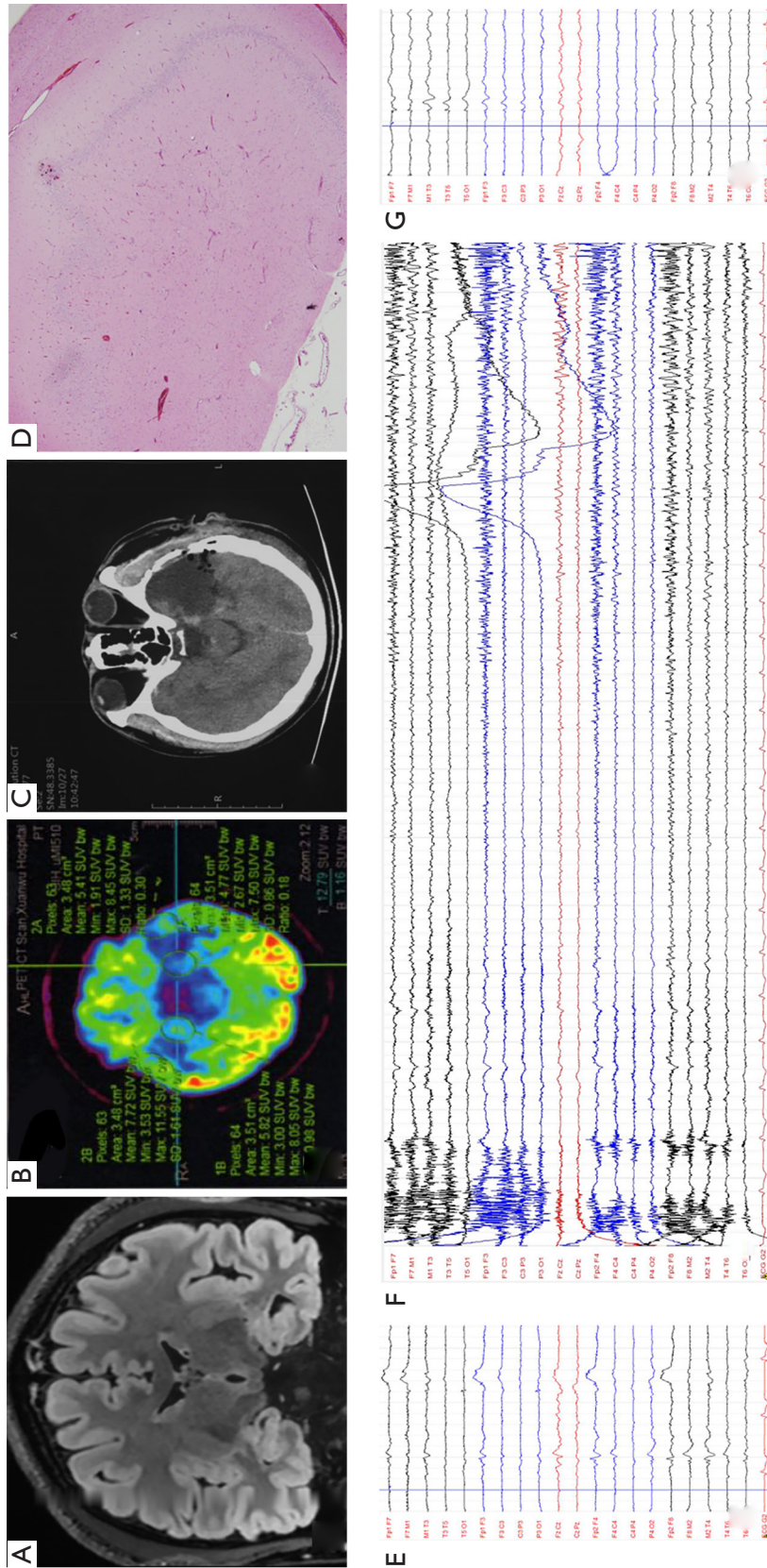


**Figure 2** Pre- and post-operation data from Pt. 10. (A) Magnetic resonance (MR) image before operation. Left hippocampal atrophy and enlargement of temporal horn are observed in fluid attenuated inversion recovery sequence; (B) preoperative positron emission tomography (PET) scan indicates that the area of low metabolism is mainly in the left medial temporal lobe (compared with the contralateral); (C) postoperative computerized tomography (CT) scan shows the range of anterior temporal lobectomy; (D) postoperative pathology indicates hippocampal sclerosis (hematoxylin-eosin staining, magnification:  $\times 40$ ); (E,F,G) scalp electroencephalogram (EEG) before surgical treatment; (E,G) indicate that the abnormal discharge is mainly distributed on the left temporal area, but there are also independent spikes and spike-slow waves in the right temporal area; (F) shows the ictal EEG, indicating that the rapid discharges at onset are mainly located on the left temporal area, while the right temporal lobe is accompanied by the synchronized rapid discharges.

**Table 2** Statistics results between ipsilateral and contralateral sides

ROIs	Ipsilateral side	Contralateral side	t/z	P
PHCR_TDI	86.26±44.7	124.1±61.25	-3.253	0.009
PHCR_QA	1.02±0.14	1.24±0.21	-4.432	0.001
PHCR_ISO	3.06±0.26	3.3±0.28	-3.752	0.004
HP_TDI	4.85±0.67	5.07±1.16	-0.753	0.469
HP_QA	1.17±0.23	1.18±0.20	-0.078	0.939
HP_ISO	3.23±0.33	3.59±0.30	-7.426	0.000022
EC_TDI	6.31±1.64	6.51±1.62	-0.474	0.646
EC_QA	0.8±0.08	0.88±0.14	-1.928	0.083
EC_ISO	2.66±0.55	3.04±0.47	-2.455	0.034
PHC_TDI	5.46±1.14	5.45±1.93	0.033	0.974
PHC_QA	0.86 (0.75, 0.9)	0.81 (0.72, 1.03)	-0.178	0.859
PHC_ISO	3.03 (2.71, 3.06)	3.19 (2.67, 3.46)	-1.824	0.068
AM_TDI	5.96±1.46	7.35±1.71	-2.844	0.017
AM_QA	1.03±0.11	1.05±0.12	-1.005	0.339
AM_ISO	3.53±0.36	4.01±0.46	-6.785	0.00048
FORX_TDI	544.41±462.02	702.57±622.17	-2.384	0.038
FORX_QA	1.92±0.5	1.99±0.44	-0.646	0.533
FORX_ISO	2.78 (2.66, 3.45)	2.81 (2.69, 3.38)	-0.089	0.929

Paired *t*-test or Wilcoxon test was used between ipsilateral and contralateral sides (PHC\_QA, PHC\_ISO, FORX\_ISO were analyzed using Wilcoxon test). PHCR, parahippocampal radiation of the cingulum; TDI, track density imaging; QA, quantitative anisotropy; FORX, fornix.

of frameless SEEG electrodes (Alcis, Besancon, France) and long-term intracranial EEG recording with definite SEEG results. Only one patient had no invasive treatment following a clear diagnosis of MTLE after MDT discussion.

Meanwhile, 11 healthy volunteers (6 men and 5 women, age: 25.1±3.5) were recruited and became the control group. There were no significant differences in age and sex between patients and controls ( $P=0.371$  and  $1.00$ ).

### Comparison between the ROIs in patients and controls

For PHCR and FORX, the quantitative analysis was first processed between the ipsilateral and contralateral sides of the patients. Our results showed that, for PHCR, the value of QA, ISO and TDI values were significantly decreased than those of the contralateral side ( $P=0.001$ ,  $0.004$ ,  $0.009$ , respectively, Paired *t*-test, Bonferroni correction). As for the FORX, the value of TDI was significantly decreased ( $P=0.038$ , Paired *t*-test, Bonferroni correction) with

another two scalars showing no difference between the two sides (Paired *t*-test for QA values and Wilcoxon for ISO values,  $P>0.05$ ). The results are displayed on *Table 2*. Next, the comparison between the patients and controls was performed. Since TDI determination was performed with a different threshold when fiber tracking and the error cannot be eliminated when comparing patients and controls (the individual tracking threshold was set at 60% of the maximum value), the QA and ISO were selected to finish the comparison. Results showed that the difference in ipsilateral PHCR\_QA and PHCR\_ISO in the patients were greatly significant compared with the volunteers (Independent-Sample *t*-test,  $P<0.05$ ), while PHCR\_QA still showing significant difference after correction for multiple comparisons ( $P<0.017$ ). When comparing the contralateral side with the control groups, there were no differences in FORX and PHCR (*Table 3* and *Table 4*). Additionally, the reconstruction of cingulum and fornix are shown as QA values on *Figure 3* and *Figure 4*.

**Table 3** Statistical results between ipsilateral side and control group

ROIs	Ipsilateral side	Control group	t/z	P
PHCR_QA	1.02±0.14	1.23±0.19	-3.291	0.002
PHCR_ISO	3.06±0.26	3.28±0.28	-2.261	0.031
HP_QA	1.17±0.23	1.23±0.19	-0.701	0.488
HP_ISO	3.23±0.33	3.54±0.32	-2.634	0.013
EC_QA	0.8±0.08	0.93±0.15	-2.615	0.014
EC_ISO	2.66±0.55	2.99±0.55	-1.602	0.119
PHC_QA	0.86 (0.75, 0.9)	0.92 (0.81, 1.18)	-1.893	0.058
PHC_ISO	3.03 (2.71, 3.06)	3.11 (2.96, 3.4)	-2.083	0.037
AM_QA	1.03±0.11	1.11±0.15	-1.655	0.108
AM_ISO	3.53±0.36	3.85±0.48	-1.901	0.067
FORX_QA	1.92±0.5	2.10±0.21	-1.17	0.265
FORX_ISO	2.78 (2.66, 3.45)	2.83 (2.74, 3.12)	-0.382	0.702

Independent-samples *t*-test or the Mann-Whitney U test was used between ipsilateral side and control group (PHC\_QA, PHC\_ISO and FORX\_ISO were calculated using Mann-Whitney U test). PHCR, parahippocampal radiation of the cingulum; QA, quantitative anisotropy; ISO, isotropic; HP, hippocampus; EC, entorhinal cortex; PHC, parahippocampus; AM, amygdala; FORX, fornix.

**Table 4** Statistical results between contralateral side and control group

ROIs	Contralateral side	Control group	t/z	P
PHCR_QA	1.24±0.21	1.23±0.19	0.074	0.941
PHCR_ISO	3.3±0.28	3.28±0.28	0.123	0.903
HP_QA	1.18±0.20	1.23±0.19	-0.669	0.508
HP_ISO	3.59±0.30	3.54±0.32	0.446	0.659
EC_QA	0.88±0.14	0.93±0.15	-0.869	0.391
EC_ISO	3.04±0.47	2.99±0.55	0.294	0.771
PHC_QA	0.81 (0.72, 1.03)	0.92 (0.81, 1.18)	-1.739	0.082
PHC_ISO	3.19 (2.67, 3.46)	3.11 (2.96, 3.4)	-0.325	0.745
AM_QA	1.05±0.12	1.11±0.15	-1.08	0.288
AM_ISO	4.01±0.46	3.85±0.48	0.91	0.370
FORX_QA	1.99±0.44	2.1±0.21	-0.787	0.446
FORX_ISO	2.81 (2.69, 3.38)	2.83 (2.74, 3.12)	-0.401	0.688

Independent-samples *t*-test or the Mann-Whitney U test was used between ipsilateral side and control group (PHC\_QA, PHC\_ISO and FORX\_ISO were calculated using Mann-Whitney U test). PHCR, parahippocampal radiation of the cingulum; QA, quantitative anisotropy; ISO, isotropic; HP, hippocampus; EC, entorhinal cortex; PHC, parahippocampus; AM, amygdala; FORX, fornix.

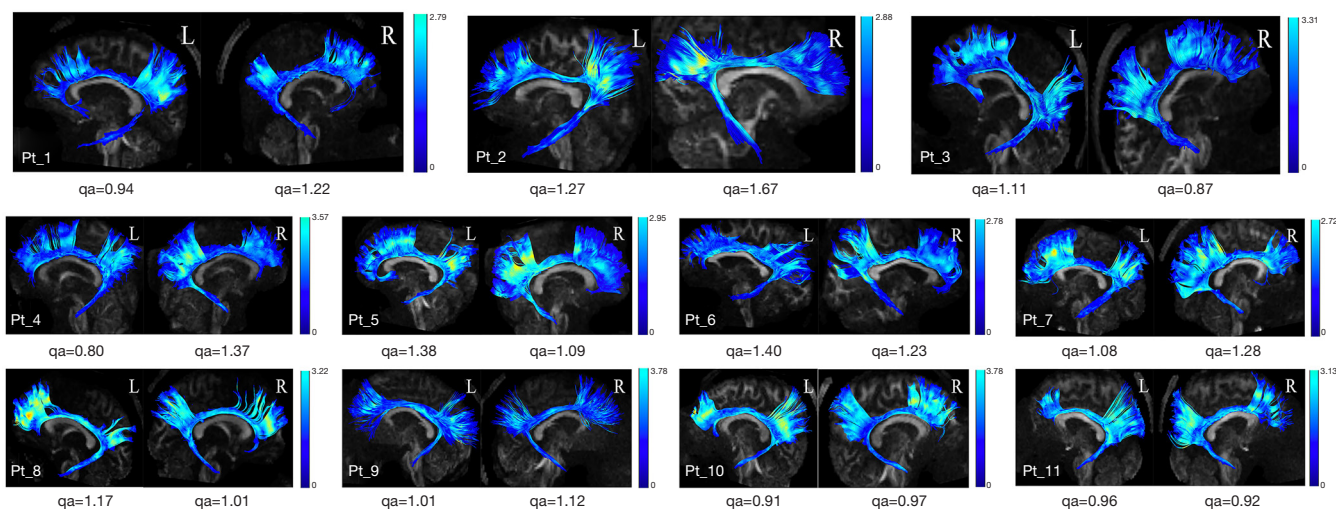


**Figure 3** Bilateral cingulum and quantitative anisotropy (QA) visualization for 11 patients. The bilateral cingulum is reconstructed and quantitatively analyzed. The QA value is visibly referenced by the color bar on DSI-Studio. The QA value on the ipsilateral side on the parahippocampal radiation of the cingulum (PHCR) area is significantly decreased.

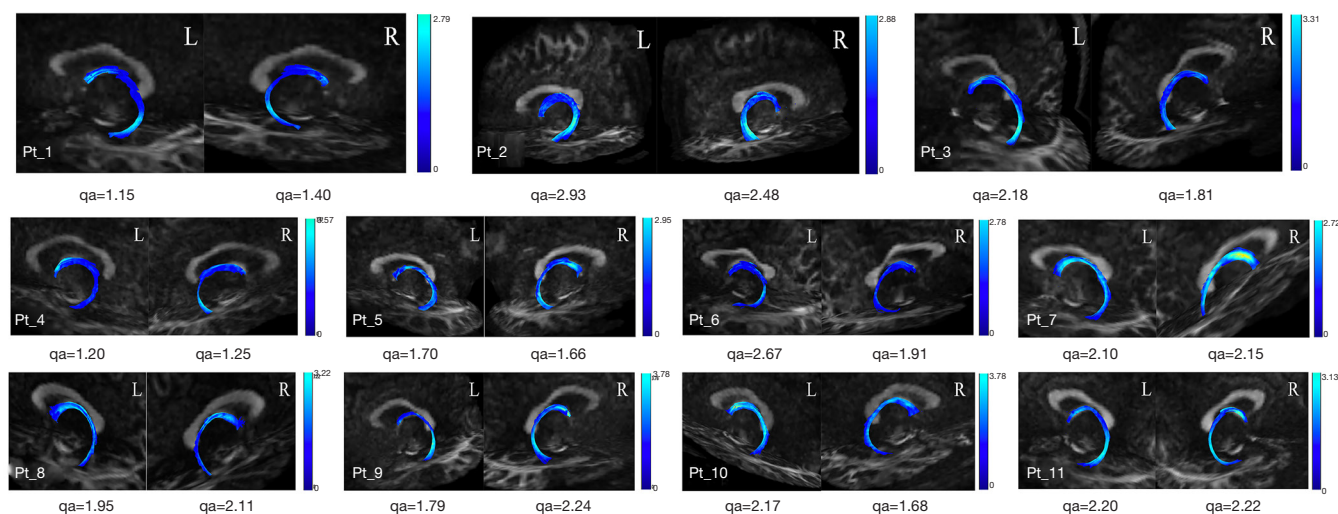


**Figure 4** Bilateral fornix and quantitative anisotropy (QA) visualization for 11 patients. The fornix is reconstructed and quantitatively analyzed following the study protocol. The QA value is visibly referenced by the color bar on DSI-Studio. The QA value on the ipsilateral side of the crus of fornix (FORX) area is significantly decreased.

As both FORX\_TDI and PHCR\_TDI measurements showed significantly decreased values in the ipsilateral side, which was better in finding the asymmetry than QA and ISO values, the comparison of sensitivity and specificity in detecting the lateralization of MTLE between FORX\_TDI and PHCR\_TDI was conducted with ROC curve for both patients and controls. There were 9/11 patients whose

pathologic findings were consistent with PHCR\_TDI abnormalities, and 0/11 healthy volunteers had PHCR\_TDI abnormalities, which indicated the sensitivity was 89.5% and specificity 100.0% for PHCR\_TDI (area under curve =0.93,  $P=0.019$ ; Table 5, Figure 5). Meanwhile, there were 10/11 patients whose pathologic findings were consistent with FORX\_TDI abnormalities, and 0/11 healthy

volunteers had FORX\_TDI abnormalities, which indicated the sensitivity was 95.0% with the specificity 100% for FORX (area under curve=0.95,  $P=0.040$ , Table 5, Figure 5). As a quantitative diffusion modality, DSI may have some advantages in finding heterogeneity between white matters. In this study, ROC curves were used to assess effectiveness of TDI scalar and comparing the sensitivity between PHCR\_TDI and FORX\_TDI. Our results showed that these two white matter structures in TDI can effectively be used to detect the lateralization of MTLE. Moreover, FORX\_TDI appeared more sensitive than PHCR\_TDI.

For the gray matter, as a matter of priority, the values of bilateral HP, PHC, AM, and EC were compared to

**Table 5** ROC analysis

AUC	Standard error	P	95% confidence interval	
			Min	Max
Test variable: PHCR_TDI				
0.930	0.058	0.019	0.816	1.000
Test variable: FORX_TDI				
0.950	0.049	0.040	0.854	1.000

ROC, receiver operating characteristic; PHCR, parahippocampal radiation of the cingulum; TDI, Track density imaging; FORX, fornix.

assess the diffusion heterogeneity between the ipsilateral and contralateral mesial temporal area. Our results showed that the values of HP\_ISO, EC\_ISO, AM\_TDI, and AM\_ISO were significantly different on the contralateral side (Paired  $t$ -test,  $P<0.05$ ). Moreover, HP\_ISO still survived after the Bonferroni method correction ( $P<0.017$ ) with the rest of the values showing a decreasing trend with no statistically significant difference (Table 2). The values of bilateral HP, PHC, AM and EC between the ipsilateral and contralateral sides and the controls were compared to further assess the heterogeneity. At first, the ipsilateral side of the four ROIs were compared with those of the control group. The results showed that the value of HP\_ISO, EC\_QA, and PHC\_ISO were significantly decreased on the ipsilateral side (Independent-Sample  $t$ -test for HP\_ISO and EC\_QA, Mann-Whitney U test for PHC\_ISO,  $P<0.05$ ). After the correction, HP\_ISO and EC\_QA showed significantly difference with the other regions showing no differences between groups ( $P<0.017$ , Table 3). Moreover, the contralateral side of the MTLE patients showed no difference when compared to that of the healthy controls (Table 4). All the statistical results can be seen in Figure 6.

## Discussion

In our study, we quantitatively demonstrated the

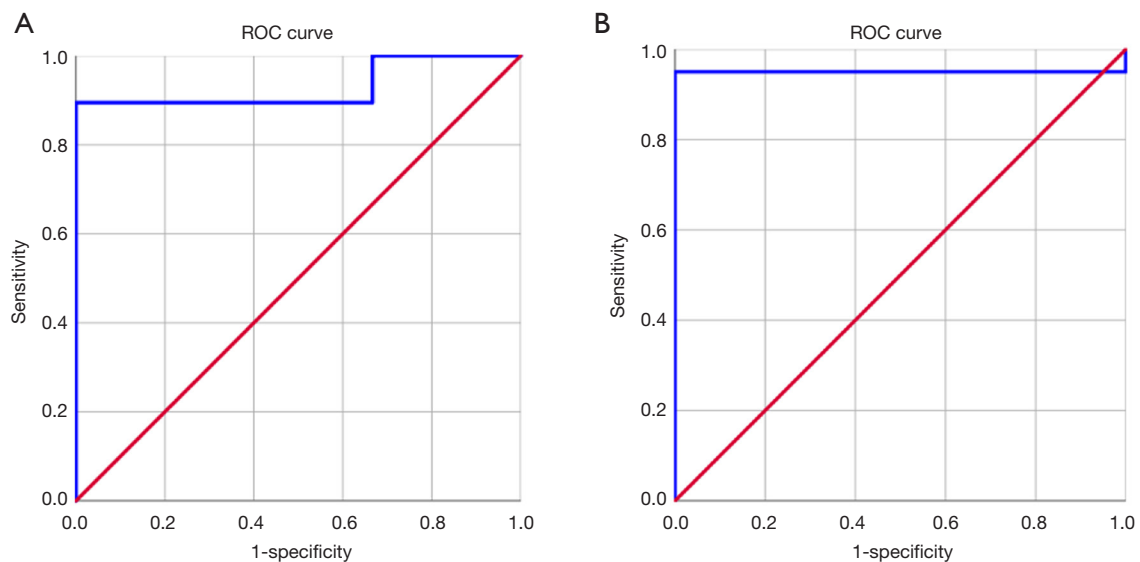


**Figure 5** ROC curve for PHCR\_TDI and FORX\_TDI. (A) The ROC curve for PHCR\_TDI shows that the area under curve was 0.93. (B) The area under curve for FORX\_TDI is 0.95, which is higher than PHCR\_TDI. PHCR, parahippocampal radiation of the cingulum; ROC, receiver operating characteristic; TDI, Track density imaging.

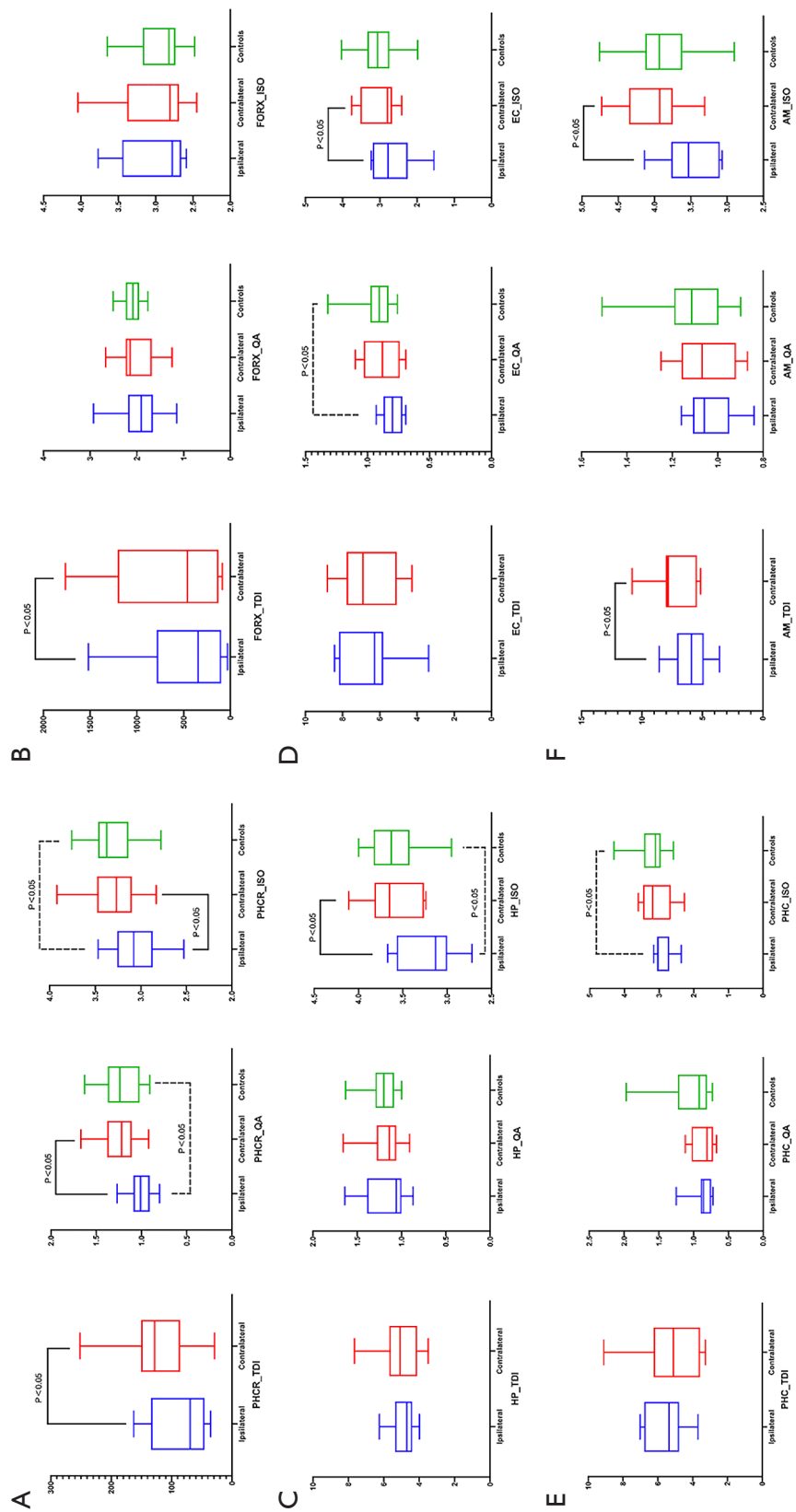


**Figure 6** Quantitative results. (A) Values of Track density imaging (TDI), quantitative anisotropy (QA), isotropic (ISO) for parahippocampal radiation of the cingulum (PHCR) are significantly decreased on the ipsilateral side ( $P < 0.05$  and  $P < 0.017$ ). (B) Results from the crus of fornix (FORX) show TDI on the ipsilateral side is lower than the contralateral side. (C) Hippocampus (HP) ISO on the ipsilateral side is significantly decreased compared to the contralateral side and the control group. (D) The value of entorhinal cortex (EC) QA on the ipsilateral side is significantly lower than the control group. (E) Results from parahippocampus (PHC) show that the values of ISO on the ipsilateral side are lower than the control group. However, the results did not survive from Bonferroni correction ( $P > 0.017$ ). (F) TDI and ISO for amygdala (AM) on the ipsilateral side are decreased compared with to contralateral side with  $P < 0.05$  and  $P < 0.017$ .

heterogeneity on the diffusion level in patients with MTLE using DSI. To the best of our knowledge, this is the first report using the GQI algorithm in DSI to quantify the diffusion differentiation between the two sides of unilateral MTLE. Based on our results, we concluded a decreased level of diffusion existed on some of the mesial temporal structures. As a preliminary exploration, DSI, with its high angular resolution may be a reliable and effective modality for the presurgical evaluation of MTLE patients.

### ***PHCR and FORX—important input and output from the HP***

In our 11 unilateral MTLE patients, significant differences were found on the bilateral PHCR and FORX. A series of decreased values were found on the ipsilateral side of the MTLE patients. The cingulum and fornix are the two important parts of the Papez circuit (17). Within the circuit, the cingulum bundle forms a collection of fibers that project from the cingulate gyrus to the EC and PHC, and this connection is reported to be associated with a series of functions such as emotion, reward, pain and memory (6,18). In contrast, the fornix forms a connection with the HP and the mammillary bodies, mainly affecting the major function of memory (19). As hippocampal sclerosis is the major pathological change in MTLE, microstructural changes in relation to the HP may occur due to the repetitive seizure attacks (1).

### ***High resolution diffusion scalar of the FROX and PHCR***

Studies focusing on cingulum and fornix have found the diffusion differences. Reports have stated the presence of widespread white and gray matter abnormalities in patients with TLE (2). Urbach *et al.* reported a reduction in the bilateral cingulum fiber in unilateral temporal lobe epilepsy with HS (6). To the best of our knowledge, most of the previously reported studies have used the technique of DTI to quantify the changes, which may lead to inaccuracy results as it only decodes the average trend of the orientation of fibers for each voxel. Lemkaddem *et al.* (2014) has used high angular resolution DSI to investigate the microstructural alterations in TLE. They found that the network topology of the unilateral TLE was less efficient to detect structural connectivity in patients compared to the control group from the aspect of structural connectivity based on the anisotropy of the diffusion (3). However, they failed to assess the diffusion heterogeneity between the

two sides in MTLE patients with the help of DSI in GQI space. Besides QA and ISO using GQI algorithm, TDI has been the preferred quantitative image reconstruction method of choice for dMRI to provide spatial resolution and anatomical information, which cannot be obtained by routine methods, especially for the white matter (14,15). In this study, we observed a significantly decreased diffusion level in the PHCR and FORX, corresponded with the microstructural changes for the white matter of MTLE patients. Moreover, the sensitivity and specificity for PHCR\_TDI and FORX\_TDI values were compared between the two structure in detecting the lateralization of MTLE. Our results showed that both ROIs in TDI had 100% specificity and higher sensitivity (89.5% and 95%, respectively) to detect the ipsilateral lateralization of MTLE. FORX in TDI tended to be more sensitive than PHCR in TDI (AUC =0.93 *vs.* AUC =0.95).

### ***Diffusion changes of the other major structures***

The diffusion level between the different subcortical structures on the bilateral side has also been quantified with DSI. As tractography is a useful method for presurgical evaluation, it is being increasingly used to investigate epilepsy, specifically TLE (4,7,20). Studies have found that on DTI, the subcortical structures, including the amygdala, HP and thalamus, ipsilateral to the seizure side, have low fractional anisotropy values (2,21-23). As DSI can resolve intravoxel diffusion heterogeneity by measuring its diffusion density spectra estimator, it tends to be more precise than DTI methods in the quantification of the diffusion level (9,24). However, no study has assessed the diffusion changes between mesial temporal gray matter structures using DSI in patients with MTLE. In our study, the diffusion level on different ROIs were significantly decreased including the HP, AM and EC in GQI space ( $P < 0.017$ ). Our preliminary results showed that although diffusion may have some advantages in finding heterogeneity between white matters, there still existed some differences between subcortical structures like HP. The diffusion level may vary in MTLE patients for both white matter and grey matter and a further investigation may be needed from the aspect of both brain networks and connection omics.

### ***Limitations***

Limitations still exist in our present study. First, the sample size we evaluated was small. There may have been some

selection bias for these data because of the small sample size. Moreover, as DSI is a newly developed imaging modality, the results presented herein are preliminary. As DSI will gradually be a routine method for both clinical and scientific use, a larger number of patients and controls may be required for further assessment. Second, in this study, we did not perform a comparison of the accuracy between DTI and DSI in lateralization of MTLE in this study. The conclusion that DSI has higher angular resolution was summarized from the previous study (24,25). A further study on simultaneously acquired DTI and DSI scans may be performed if necessary. Finally, other parts of the ROIs such as the uncinate gyrus were not included in our comparisons and need to be further investigated in our future studies.

## Conclusions

We have compared the diffusion differences between patients with MTLE and healthy controls using highly angular DSI with GQI algorithm in unilateral MTLE. We investigated the heterogeneity in both gray and white matters between the two sides and found that the quantitative diffusion scalars of the DSI are sufficiently sensitive to define the ipsilateral lateralization of MTLE during the presurgical evaluations. As a preliminary result, this quantitative technique may play a supplementary noninvasive role in presurgical assessment of MTLE patients, especially in cases when conventional MRI findings tends to be negative.

## Acknowledgments

The authors want to thank all the volunteers who participated in this study. We also want to thank our colleagues from the Department of Radiology, Xuanwu Hospital, for offering the assistance with data processing.

*Funding:* This work was supported by the National Natural Science Foundation of China (Grant Numbers 81801288, 81871009) and Green Seedling Plan, Beijing Municipal Administration of Hospitals (QML20190805).

## Footnote

*Reporting Checklist:* The authors have completed the STROBE reporting checklist. Available at <http://dx.doi.org/10.21037/atm-20-5719>

*Data Sharing Statement:* Available at <http://dx.doi.org/10.21037/atm-20-5719>

<http://dx.doi.org/10.21037/atm-20-5719>

*Conflicts of Interest:* All authors have completed the ICMJE uniform disclosure form (available at <http://dx.doi.org/10.21037/atm-20-5719>). The authors have no conflicts of interest to declare.

*Ethical Statement:* The authors are accountable for all aspects of the work in ensuring that questions related to the accuracy or integrity of any part of the work are appropriately investigated and resolved. The study was conducted in accordance with the Declaration of Helsinki (as revised in 2013). The study was approved by the ethics committee at Xuanwu Hospital (NO. LYS [2019] 097) and informed consent was taken from all the patients.

*Open Access Statement:* This is an Open Access article distributed in accordance with the Creative Commons Attribution-NonCommercial-NoDerivs 4.0 International License (CC BY-NC-ND 4.0), which permits the non-commercial replication and distribution of the article with the strict proviso that no changes or edits are made and the original work is properly cited (including links to both the formal publication through the relevant DOI and the license). See: <https://creativecommons.org/licenses/by-nc-nd/4.0/>.

## References

1. Scanlon C, Mueller SG, Cheong I, et al. Grey and white matter abnormalities in temporal lobe epilepsy with and without mesial temporal sclerosis. *J Neurol* 2013;260:2320-9.
2. Bao Y, He R, Zeng Q, et al. Investigation of microstructural abnormalities in white and gray matter around hippocampus with diffusion tensor imaging (DTI) in temporal lobe epilepsy (TLE). *Epilepsy Behav* 2018;83:44-9.
3. Lemkaddem A, Daducci A, Kunz N, et al. Connectivity and tissue microstructural alterations in right and left temporal lobe epilepsy revealed by diffusion spectrum imaging. *Neuroimage Clin* 2014;5:349-58.
4. Pustina D, Avants B, Sperling M, et al. Predicting the laterality of temporal lobe epilepsy from PET, MRI, and DTI: A multimodal study. *Neuroimage Clin* 2015;9:20-31.
5. Shih YC, Tseng CE, Lin FH, et al. Hippocampal Atrophy Is Associated with Altered Hippocampus-Posterior Cingulate Cortex Connectivity in Mesial Temporal Lobe Epilepsy with Hippocampal Sclerosis. *AJNR Am J*

- Neuroradiol 2017;38:626-32.
6. Urbach H, Egger K, Rutkowski K, et al. Bilateral cingulum fiber reductions in temporal lobe epilepsy with unilateral hippocampal sclerosis. *Eur J Radiol* 2017;94:53-7.
  7. Nazem-Zadeh MR, Elisevich K, Air EL, et al. DTI-based response-driven modeling of mTLE laterality. *Neuroimage Clin* 2015;11:694-706.
  8. Fernández-Miranda JC, Rhoton AL Jr, Alvarez-Linera J, et al. Three-dimensional microsurgical and tractographic anatomy of the white matter of the human brain. *Neurosurgery*. 2008;62:989-1026; discussion 1026-8.
  9. Wedeen VJ, Hagmann P, Tseng WY, et al. Mapping complex tissue architecture with diffusion spectrum magnetic resonance imaging. *Magnetic Resonance in Medicine* 2005;54:1377-86.
  10. Johansen-Berg H, Rushworth MF. Using diffusion imaging to study human connective anatomy. *Annu Rev Neurosci* 2009;32:75-94.
  11. Schmahmann JD, Pandya DN, Wang R, et al. Association fibre pathways of the brain: parallel observations from diffusion spectrum imaging and autoradiography. *Brain* 2007;130:630-53.
  12. Yeh FC, Wedeen VJ, Tseng WY. Estimation of fiber orientation and spin density distribution by diffusion deconvolution. *Neuroimage* 2011;55:1054-62.
  13. Nigro S, Barbagallo G, Bianco MG, et al. Track density imaging: A reliable method to assess white matter changes in Progressive Supranuclear Palsy with predominant parkinsonism. *Parkinsonism Relat Disord* 2019;69:23-9.
  14. Dai JK, Wang SX, Shan D, et al. Super-Resolution Track-Density Imaging Reveals Fine Anatomical Features in Tree Shrew Primary Visual Cortex and Hippocampus. *Neurosci Bull* 2018;34:438-48.
  15. Calamante F, Tournier JD, Jackson GD, et al. Track-density imaging (TDI): super-resolution white matter imaging using whole-brain track-density mapping. *Neuroimage* 2010;53:1233-43.
  16. Fisher RS, Cross JH, D'Souza C, et al. Instruction manual for the ILAE 2017 operational classification of seizure types. *Epilepsia* 2017;58:531-42.
  17. Papez JW. A proposed mechanism of emotion. 1937. *J Neuropsychiatry Clin Neurosci* 1995;7:103-12.
  18. Bubb EJ, Metzler-Baddeley C, Aggleton JP. The cingulum bundle: Anatomy, function, and dysfunction. *Neurosci Biobehav Rev* 2018;92:104-27.
  19. Garcia-Bengochea F, Corrigan R, Morgane P, et al. Studies on the function of the temporal lobes. I. The section of the fornix. *Trans Am Neurol Assoc* 1951;56:238-9.
  20. Stylianou P, Hoffmann C, Blat I, et al. Neuroimaging for patient selection for medial temporal lobe epilepsy surgery: Part 1 Structural neuroimaging. *J Clin Neurosci* 2016;23:14-22.
  21. Salmenpera TM, Simister RJ, Bartlett P, et al. High-resolution diffusion tensor imaging of the hippocampus in temporal lobe epilepsy. *Epilepsy Res* 2006;71:102-6.
  22. Thivard L, Lehericy S, Krainik A, et al. Diffusion tensor imaging in medial temporal lobe epilepsy with hippocampal sclerosis. *Neuroimage* 2005;28:682-90.
  23. Hakyemez B, Erdogan C, Yildiz H, et al. Apparent diffusion coefficient measurements in the hippocampus and amygdala of patients with temporal lobe seizures and in healthy volunteers. *Epilepsy Behav* 2005;6:250-6.
  24. Fernandez-Miranda JC, Pathak S, Engh J, et al. High-definition fiber tractography of the human brain: neuroanatomical validation and neurosurgical applications. *Neurosurgery* 2012;71:430-53.
  25. Maier-Hein KH, Neher PF, Houde JC, et al. The challenge of mapping the human connectome based on diffusion tractography. *Nat Commun* 2017;8:1349.

**Cite this article as:** Wang YH, Wang ZM, Wei PH, Lu C, Fan XT, Ren LK, Shan YZ, Lu J, Zhao GG. Lateralizing the affected side of hippocampal sclerosis with quantitative high angular resolution diffusion scalars: a preliminary approach validated by diffusion spectrum imaging. *Ann Transl Med* 2021;9(4):297. doi: 10.21037/atm-20-5719